

High Efficiency and Quick Response of Torque Control for a Multi-Phase Machine Using Discrete/Continuous Approach: Application to Five-phase Permanent Magnet Synchronous Machine

Abstract. This article presents a hybrid control strategy (Discrete/Continuous) for controlling the five-phase permanent magnet synchronous machine powered by a voltage inverter. The hybrid aspect of this approach comes from the fact of taking into account the voltage inverter and the machine in a unified manner during the modelling process, i.e. modelling includes at the same time continuous and discrete variables. Simulation results performed under Matlab/Simulink are presented and discussed for the purpose of the performances verification of the proposed control strategy. The obtained results will show in particular the principal advantages of the adopted control strategy like the enhancement of the dynamic torque response of this machine, and the oscillations' minimization of controlled parameters such as torque and current.

Streszczenie. W artykule zaprezentowano hybrydową strategię sterowania pięciofazowym silnikiem synchronicznym z magnesami trwałymi. Silnik zasilany jest z wykorzystaniem przekształtnika. Przedstawiono wyniki symulacji systemu. Otrzymano poprawę dynamiki momentu i zmniejszenie oscylacji. (Sterowanie wielofazowym silnikiem z wykorzystaniem strategii hybrydowej – dyskretno/ciągłej)

Keywords: Discrete/Continuous approach; Hybrid control; Multi-phase machine; Multi-phase Machine ; Five-phase permanent magnet synchronous machine.

Słowa kluczowe: silnik pięciofazowy, silnik synchroniczny, sterowanie hybrydowe

Introduction

In recent years, interest in multiphase machines has been increased due to the offered advantages over the three-phase machines [1-11], such as power splitting, therefore reducing stress on components, also the reducing the torque ripples and operating in degraded mode [1-7,9-15]. This kind of machines can be used for automotive electric traction, marine electric propulsion, wind turbines or high power industrial electrical applications [1-7,11-14].

In all these applications, the knowledge and mastering of the torque is very important. However, for an efficient control of the torque dynamics, more advanced and developed control strategies must be employed. The commonly used command is the vector control which allows the control of torque transients. Nevertheless, the performances of this command are often limited due to the non-linearity and variations in system parameters [16-18].

A control strategy, which is known as Direct Torque Control (DTC), has appeared to be competitive with the vector control techniques. In contrast to the latter, it is less sensitive to parametric variations of the machine and it allows obtaining a precise and fast torque dynamic [11,17-20]. The control principle is meant to directly control the torque and stator flow of the machine. In this context, two hysteresis comparators enable comparing the estimated values with those of the used references, then the inverter states are directly controlled through a predefined selection table [2, 3, 14, 17, 18, 20-24]. This strategy has two major disadvantages: on one hand, the switching frequency is highly variable and on the other hand, the waves amplitude of the torque and the stator flux remain less controlled over the entire speed range of the planned operation [3, 11,14, 17-19, 22-24].

In DTC structure, the converter-machine assembly is a hybrid dynamic system whose continuous part is the machine and the discrete part is the voltage inverter. This constraint has led to the development of a new control method proposed in [25-30], named «Hybrid Control», based on a Hybrid Dynamic Systems (HDS) class model, i.e. modeling includes at the same time continuous and discrete variables [31-36]. In this sense, the "discrete"

behavior of the voltage inverter and the "continuous" behavior of the machine are taken into account in a unified manner, This control presents interesting dynamic performances and does not require neither hysteresis controller nor an implementation of an observer [25-30] making it an alternative solution to avoid the disadvantages of the conventional DTC. This control is applied to a large category of systems proposed in [25-30], and recently to multicellular converters [34, 37-40].The diversity in application domains is based on a unique principle of the prediction of the phenomenon. This principal can be summarized in the following five steps:

The general model determination of the set of energy modulator behavior and the continuous process, taking into account the continuous and discrete variables of the system.

$$(1) \quad \dot{x}(t) = f(x(t), u_j(t)) \quad j \in \{1, 2, \dots, n\}$$

The integration of (1) by the Euler method over a short time interval T.

$$(2) \quad x(t + T) = x(t) + T \cdot f(x(t), u_j(t))$$

Searching for the linearity domain in which the trajectories in the state space are rectilinear. This constraint implies the determination of the maximum decision time τ_{max} and a minimum time τ_{min} , the latter is a function of temporal execution constraints, material and computing capacity.

From a measured state $x(t)$, we determine the possible directions d_j in the state space relative to the different command states

$$(3) \quad d_j = x(t + T) - x(t) = T \cdot f(x(t), u_j(t))$$

Choosing the closest direction to the reference state, then applying the corresponding configuration to the chosen direction during an optimized time by respecting the constraint of linearity of the trajectories.

In this favorable context, the presented work in this article aims at improving and applying this hybrid approach to the torque control of five-phase permanent magnet

synchronous machine, this machine is equivalent to the combination of three fictitious machines; main, secondary and homopolar [41]. Only the currents of the main fictitious machine contribute to the creation of the electromagnetic torque [10, 42-44]. The currents of the secondary fictitious machine are the cause of undesirable harmonics [10, 42-44]. This consequence is used to control the voltage inverter. Within the five-phase inverter, 32 combinations are possible. These combinations permit to generate 32 positions of the voltage vector; 2 positions correspond to the zero vector. The projections of the other 30 vectors in the fictitious plans (main and secondary) form a small, medium and large decagon for each plan, each one of them is composed of 10 vectors, the vectors that form the large decagon in one plan form the small decagon in the other, and the vectors that form the medium decagons in the two plans are identical [2,6,14, 42].

For controlling a five phase inverter, the objective is to generate the correct voltage necessary in the main plan and to generate the smallest possible voltages in the other secondary plan. In this case, only the large decagon vectors of the main plan and zero vectors are used [2]. However, the active vector in the main plan is not cancelled in the secondary plan and consequently the third order (3) harmonics are present. This problem can be resolved by applying medium and large decagon vectors in the main plan such that the medium and small vectors cancel each other in the secondary plan [6, 45-46].

For the application of the proposed control on the Five-phase Permanent Magnet Synchronous Machine, we determine the possible directions d_j in the state space relative to the different states of the superior polygon in the principal plan and the vectors that have a zero projection; then we select the closest direction to the reference state, and calculate the application time of the configuration corresponding to the chosen direction; Deducing the application times of the medium and large vector.

The obtained model was simulated using Matlab/Simulink software, and the simulation results are presented and discussed to verify the performances of the studied control strategy.

Modeling of the five-phase permanent magnet synchronous machine

The Park model of the five-phase permanent magnets synchronous machine is defined by the following system of equations [10]:

$$(4) \quad \begin{cases} v_{dp} = R_s I_{dp} + L_p \frac{dI_{dp}}{dt} - \omega L_p I_{qp} \\ v_{qp} = R_s I_{qp} + L_p \frac{dI_{qp}}{dt} + \omega L_p I_{dp} + \sqrt{\frac{5}{2}} \Phi_f \omega \\ v_{ds} = R_s I_{ds} + L_s \frac{dI_{ds}}{dt} \\ v_{qs} = R_s I_{qs} + L_s \frac{dI_{qs}}{dt} \end{cases}$$

The mechanical equation is written:

$$(5) \quad J \cdot \frac{d\omega}{dt} = T_{em} - T_r - f \cdot \omega$$

The electromagnetic torque is given by:

$$(6) \quad T_{em} = \sqrt{\frac{5}{2}} p \cdot \Phi_f \cdot i_{qp}$$

Five-phase inverter Modeling

Figure (1) shows the structure of a five-phase inverter [2,6]. Each arm of the inverter can be presented by a two-position switch.

The inverter switches are considered ideal. The switches states are represented by a vector of dimension (5×1) in equation (7):

$$(7) \quad [S] = \begin{bmatrix} S_a \\ S_b \\ S_c \\ S_d \\ S_e \end{bmatrix}$$

The phases voltages as a function of the conduction state of the inverter are expressed by:

$$(8) \quad [V] = \begin{bmatrix} V_a \\ V_b \\ V_c \\ V_d \\ V_e \end{bmatrix} = \frac{v_0}{5} \begin{bmatrix} 4 & -1 & -1 & -1 & -1 \\ -1 & 4 & -1 & -1 & -1 \\ -1 & -1 & 4 & -1 & -1 \\ -1 & -1 & -1 & 4 & -1 \\ -1 & -1 & -1 & -1 & 4 \end{bmatrix} \cdot \begin{bmatrix} S_a \\ S_b \\ S_c \\ S_d \\ S_e \end{bmatrix}$$

The combinations of the 5 states $(S_a S_b S_c S_d S_e)$ allow generating 32 positions of the vector $[V]$ of which 2 correspond to the zero vector: $(S_a S_b S_c S_d S_e) = (0 0 0 0 0)$ or $(1 1 1 1 1)$ [6].

The projections of stator voltage vectors in each is considered fictitious plan are shown in figure 2 and 3. [2, 6, 14].

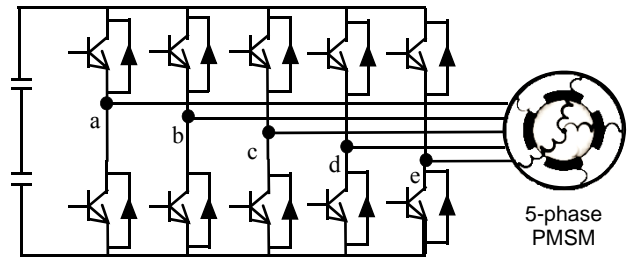


Fig.1. Example of a five-phase inverter for the five-phase synchronous machine.

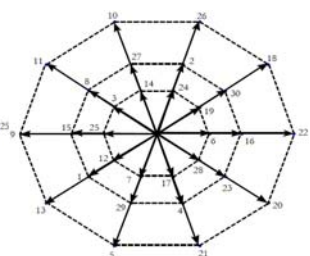
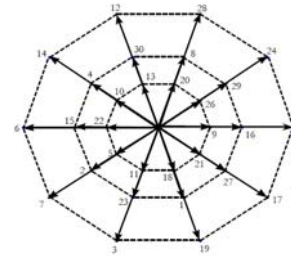


Fig.2. Projection of voltage vectors in the main plan Fig.3. Projection of voltage vectors in the secondary plan

The control Algorithm

The five-phase machine is equivalent to three fictitious sub-machines, magnetically decoupled and mechanically coupled.

In the case of machines with sinusoidal flux distribution, only the first fictitious machine M1 produces an electromotive force voltage (EMF) [2, 42-44]. Thus, it is the only one to produce an electromagnetic torque [2, 42-44]. In this case, the objective is to generate the correct voltage reference in the principal machine and to generate the smallest possible voltages in the other fictitious machines.

In this case for the inverter, we employ only the vectors that have a null projection and the group of vectors of the same standard that represents the superior polygon in the main plan [2].

However, the use of the vectors of the large decagon alone will create the third order harmonic, resulting in a distortion of the waveforms; this is not desirable since we are interested in waveforms that are very close to sinusoids.

Therefore, the medium and large vectors are the ones to be applied by assigning to each one a well-defined period of time in order to cancel the temporal averages in the secondary plan Fig.4 [45-46].

The electromagnetic torque is proportional to the current i_{qp} . In the state space, the current references are $i_{dp}^* = 0$ (to minimize the joule losses) i_{qp}^* proportional to the torque set point [26, 27].

The hybrid control algorithm involves monitoring the reference currents i_{dp}^* i_{qp}^* , in the state space i_{dp} i_{qp} . It is summarized by the following processing sequences:

- The determination of the hybrid model of the converter-machine assembly based on the main plan;
- The calculation of the possible directions in the state space relative to the different states of the superior polygon in the principal plan and the vectors that have a zero projection;
- The choice of the closest direction to the reference state;
- The calculation of the application time of the configuration corresponding to the chosen direction;
- Deducing the application times of the medium and large vector.

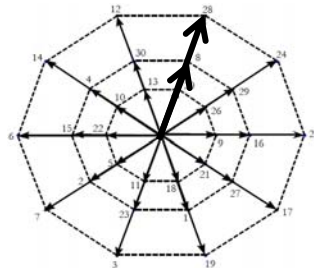


Fig.4.a. Representation of the active vectors in both plan principal

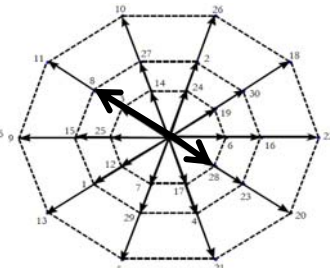


Fig.4.b. Representation of the active vectors in both plan secondary

1. Hybrid model of the behavior of the inverter-machine assembly

From equation (4), the main machine model can be modeled by a state representation in the following form:

(9)

$$\frac{d}{dt} \begin{bmatrix} i_{dp} \\ i_{qp} \end{bmatrix} = \begin{bmatrix} -\frac{R}{L_{dp}} & \frac{L_{qp}}{L_{dp}} \cdot \omega \\ -\frac{L_{dp}}{L_{qp}} \cdot \omega & -\frac{R}{L_{qp}} \end{bmatrix} \cdot \begin{bmatrix} i_{dp} \\ i_{qp} \end{bmatrix} + \begin{bmatrix} \frac{1}{L_{dp}} & 0 \\ 0 & \frac{1}{L_{qp}} \end{bmatrix} \cdot \begin{bmatrix} V_{dp} \\ V_{qp} \end{bmatrix} - \sqrt{\frac{5}{2}} \cdot \frac{\omega}{L_{dp}} \cdot \begin{bmatrix} 0 \\ \Phi_{fp} \end{bmatrix}$$

The stators voltage can be expressed by:

$$(10) \quad \begin{bmatrix} V_{dp} \\ V_{qp} \end{bmatrix} = [P(\theta)] \frac{v_0}{5} \begin{bmatrix} 4 & -1 & -1 & -1 & -1 \\ -1 & 4 & -1 & -1 & -1 \\ -1 & -1 & 4 & -1 & -1 \\ -1 & -1 & -1 & 4 & -1 \\ -1 & -1 & -1 & -1 & 4 \end{bmatrix} \cdot \begin{bmatrix} S_a \\ S_b \\ S_c \\ S_d \\ S_e \end{bmatrix}$$

(11)

$$[P(\theta)] = \sqrt{\frac{2}{5}} \begin{bmatrix} \cos(\theta) & \cos(\theta - \frac{2\pi}{5}) & \cos(\theta - \frac{4\pi}{5}) & \cos(\theta - \frac{6\pi}{5}) & \cos(\theta - \frac{8\pi}{5}) \\ \sin(\theta) & \sin(\theta - \frac{2\pi}{5}) & \sin(\theta - \frac{4\pi}{5}) & \sin(\theta - \frac{6\pi}{5}) & \sin(\theta - \frac{8\pi}{5}) \end{bmatrix}$$

We insert equation (9) in equation (10), the hybrid model of our system can be written in a form of equation (3) as follow:

$$(12) \quad \dot{x}(t) = f(x, u_j) = A \cdot x + B \cdot u_j + D$$

with:

$$x = \begin{bmatrix} i_{dp} \\ i_{qp} \end{bmatrix}; u_j = \begin{bmatrix} S_a \\ S_b \\ S_c \\ S_d \\ S_e \end{bmatrix}; A = \begin{bmatrix} -\frac{R}{L_{dp}} & \omega \\ -\omega & -\frac{R}{L_{qp}} \end{bmatrix};$$

$$B = \begin{bmatrix} \frac{1}{L_{dp}} & 0 \\ 0 & \frac{1}{L_{qp}} \end{bmatrix} \cdot [P(\theta)] \frac{v_0}{5} \begin{bmatrix} 4 & -1 & -1 & -1 & -1 \\ -1 & 4 & -1 & -1 & -1 \\ -1 & -1 & 4 & -1 & -1 \\ -1 & -1 & -1 & 4 & -1 \\ -1 & -1 & -1 & -1 & 4 \end{bmatrix};$$

$$D = -\sqrt{\frac{5}{2}} \cdot \frac{\omega}{L_{dp}} \cdot \begin{bmatrix} 0 \\ \Phi_{fp} \end{bmatrix}$$

2. Determination of the directions

The control algorithm calculates, for a measured state, the directions d_j in the state space that correspond to the different states of the control u_j of the large decagon in the principal plan and the vectors that have a zero projection, using equation (3).

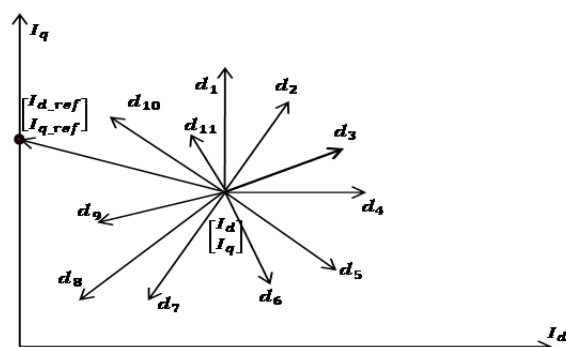


Fig.5. Example of possible directions

3. The choice of direction

Among the 11 directions, the chosen direction is the one with direction that forms the smallest angle with respect to the desired direction [25-30].

$$(13) \quad (\vec{d}_{ch}, \vec{d}_{ref}) = \min_{1 < j < 11} (\vec{d}_j, \vec{d}_{ref})$$

with

$$(14) \quad (\vec{d}_j, \vec{d}_{ref}) = \cos^{-1} \left(\frac{\vec{d}_j \cdot \vec{d}_{ref}}{\|\vec{d}_j\| \cdot \|\vec{d}_{ref}\|} \right)$$

4. Calculation of the application time of the configuration that correspond to the chosen direction

The application time of the chosen configuration is determined from the length of the projection vector of the desired direction on the chosen direction [25-30], and it is written as follows:

$$(15) \quad t = \frac{T \cdot \|\vec{d}_{ref}\| \cdot \cos((\vec{d}_{chois\acute{e}e}, \vec{d}_{ref}))}{\|\vec{d}_{chois\acute{e}e}\|}$$

5. Deducing the application times of the medium and large vector

The application times of the medium and large vector are calculated in the main plan as shown below:

$$(16) \quad t \cdot V_1 = t_1 \cdot V_1 + t_m \cdot V_m$$

$$(17) \quad t_1 \cdot V_s = t_m \cdot V_m$$

Where V_s , V_m and V_1 represent respectively the amplitude of the small, medium and large vector, are given as follows:

$$(18) \quad V_s = \frac{2}{5} V_{dc} 2\cos(\frac{\pi}{5}), V_m = \frac{2}{5} V_{dc}, V_1 = \frac{2}{5} V_{dc} 2\cos(\frac{2\pi}{5})$$

From equations (15), (16), (17) and (18), the periods t_l and t_m are written as follows:
(19)

$$\begin{cases} t_l = \frac{0.7236 \cdot T \cdot \|\vec{d}_{ref}\| \cdot \cos(\angle(\vec{d}_{chois\acute{e}e}, \vec{d}_{ref}))}{\|\vec{d}_{chois\acute{e}e}\|} \\ t_m = \frac{0.2764 \cdot T \cdot \|\vec{d}_{ref}\| \cdot \cos(\angle(\vec{d}_{chois\acute{e}e}, \vec{d}_{ref}))}{\|\vec{d}_{chois\acute{e}e}\|} \end{cases}$$

Simulation results and interpretation

We have simulated the operation of the inverter-machine assembly using MATLAB/Simulink software.

The used machine has the following characteristics:

$$R_s = 0.12\Omega; L_d = L_q = 1.35\text{mH}; \Phi_f = 0.05 \text{ Wb}; p = 4$$

The simulation results shown in figure 6 concern the steady-state operation of the five-phase permanent magnet synchronous machine. For the set point of i_{q_ref} equal to the nominal current ($i_{q_ref} = 5\text{A}$), it is a reference i_{sd_ref} zero.

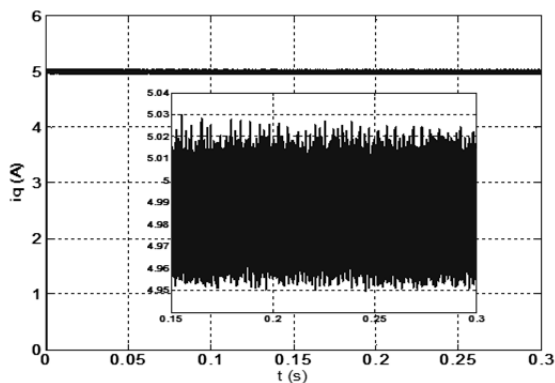


Fig.6.a. Stator current i_q

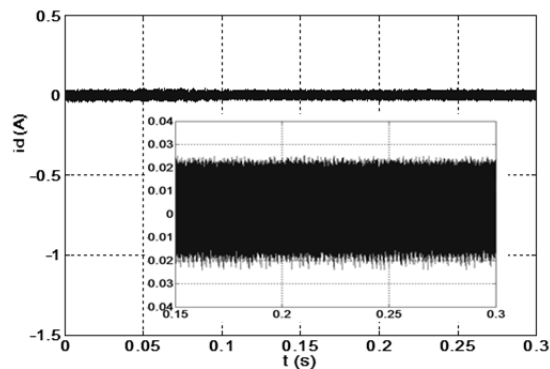


Fig.6.b. Stator current i_d

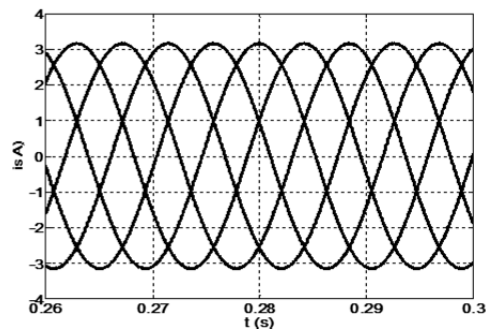


Fig.6.c. Phases currents

Fig.6. Simulation results of the steady state control.

Figures (6.a and b) illustrate the temporal variation of the i_q and i_d currents, we can observe that the i_q current immediately attains its reference value of 5 A with a slight oscillatory deviation of 0.07 A of amplitude around its reference value. The i_d current control is more accurate with 0.04 A oscillation.

The steady state phase currents have been illustrated in Fig. (6.c), we notice that these currents look like sinusoids with low noise.

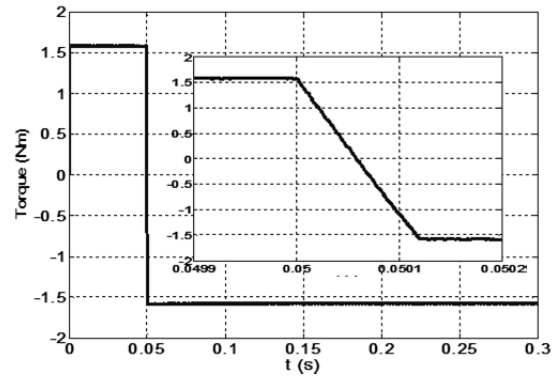


Fig.7.a. Electromagnetic torque

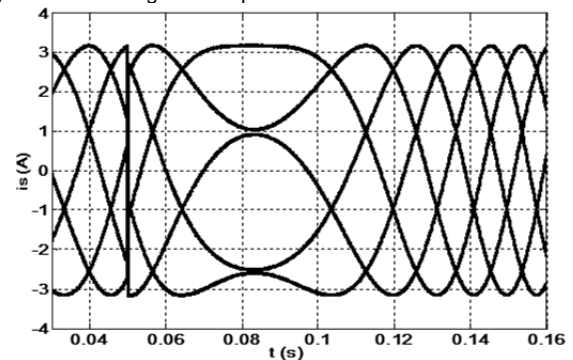


Fig.7.b. Phases currents

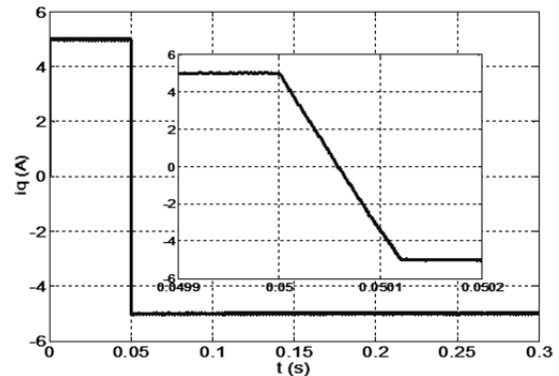


Fig.7.c. Stator current i_q

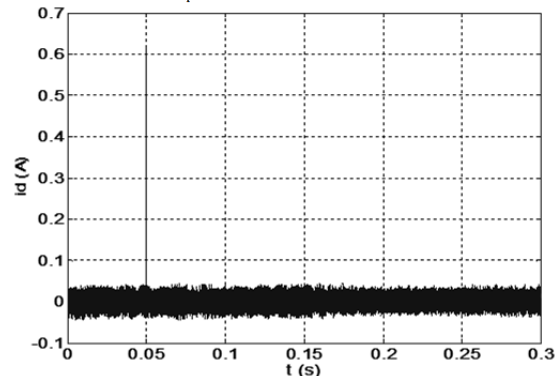


Fig.7.d. Stator current i_d

Fig.7. Simulation results of the control in transient state.

For the study of the transient state, an abrupt reversal of the set point is applied. We observe that the torque inversion is extremely fast (less than 200 μ s) and is carried out without a significant impact Figure (7.a).

In order to have a better appreciation of the obtained results, we have compared with that of the classical vector control. By presenting the responses of the torque for the two controls (hybrid control and Field Oriented Control (FOC-SVM)) in the same figure 8. The comparison of these results shows that the hybrid control shows very high dynamics and precision of response of the torque, indeed contrary to the FOC-SVM control.

The phase currents are remarkably well controlled during the transient state and they do not exceed any limits and do not lead to any over current Figures (7.b), contrary to the FOC-SVM control where the current exceeds the set value figure 9.

From the figures (7.c and d), it can be seen that the i_d and i_q currents are well adjusted; therefore, the control is robust regarding sudden variation in the set-point. Where the i_d current is maintained at zero and follows the set-point during entire operating cycle. Concerning the FOC-SVM control, one can note the effect of recoupling on the current i_d during this change, which induces a slower response time figure 10.

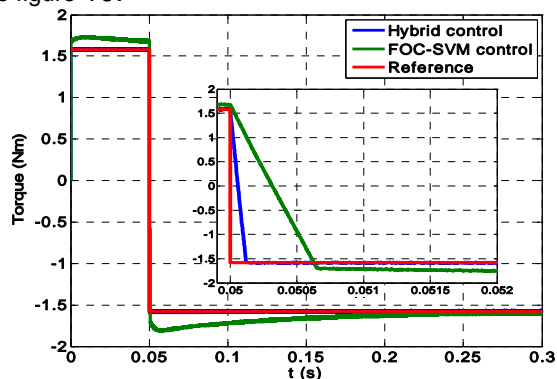


Fig.8. Torque evolution for both controls

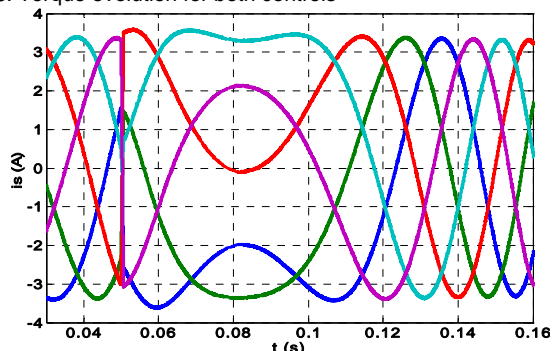


Fig.9. Currents of phases in the case of FOC-SVM

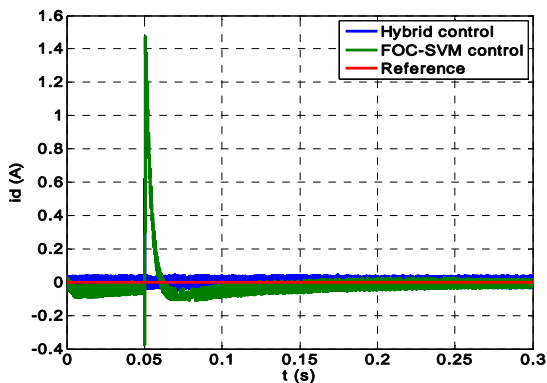


Fig.10. Current i_d for both controls

Conclusion

A Hybrid Direct Torque Control, based on a formal representation of inverter-machine behavior, has been developed and applied to a Five-phase Permanent Magnet Synchronous Machine. The control scheme provides good torque dynamic performances, and no observer or estimator is necessary. In the context of the machine control by means of an inverter, the Hybrid Control Torque is regulated directly at the inverter switches level. Also this control makes it possible to reduce the number of regulators and to have excellent dynamic performances.

Authors: Dr Djamel DIFI, Process Control Laboratory, National Polytechnic School, Algiers, Algeria, E-mail: d.difi@yahoo.fr.
Dr Khaled HALBAOUI, Power Electronics Laboratory, Nuclear Research Centre of Brine CRNB, Djelfa, Algeria, E-mail: halbaoui_khaled@crnb.dz.
Prof Djamel BOUKHETALA, Process Control Laboratory, National Polytechnic School, Algiers, Algeria, E-mail: dboukhetala@yahoo.fr

REFERENCES

- [1] Arahali. M.R, Barrero. F, Toral. S, Duran. M, Gregor. R. Multi-phase current control using finite-state model-predictive control. *Control Engineering Practice* 2009; 17: 579–587.
- [2] Echeikh. H, Trabelsi. R, Iqbal. A, Mimouni.M.F. Adaptive direct torque control using Luenberger-sliding mode observer for online stator resistance estimation for five-phase induction motor drives. *Electrical Engineering*. September 2018, Volume 100, Issue 3, pp 1639–1649.
- [3] Abjadi. N.R. Sliding-mode control of a six-phase series/parallel connected two induction motors drive. *ISA Transactions* 2014; 53: 1847-1856.
- [4] Hosseini. A, Trabelsi. R, Mimouni. M.F, Iqbal. A, Alammari. R. Sensorless sliding mode observer for a five-phase permanent magnet synchronous motor drive. *ISA Transactions* 2015; 58: 462-473.
- [5] IQBAL. A, SINGH. GK, PANT. V. Stability analysis of an asymmetrical six-phase synchronous motor. *Turk J Elec Eng & Comp Sci* 2016; 24: 1674-1692.
- [6] Saleh. K, Sumner. M. Sensorless speed control of five-phase PMSM drives with low current distortion. *Electrical Engineering*. June 2018, Volume 100, Issue 2, pp 357–374
- [7] Wang. X, Wang. Z, Xu. Z. A Hybrid Direct Torque Control Scheme for Dual Three-phase PMSM Drives with Improved Operation Performance. *IEEE Transactions on Power Electronics*. 2018; 63: 321–333.
- [8] Echeikh. H, Trabelsi. R, Iqbal. A, Bianchi. N, Mimouni. M.F. Non-linear control of five-phase IM drive at low speed conditions—experimental implementation. *ISA Transactions* 2016; 65: 244-253
- [9] Bermudez. M, Gomozov. O, Kestelyn. X, Barrero. F, Nguyen. N.K., Semail. E. Model predictive optimal control considering current and voltage limitations: Real-time validation using OPAL-RT technologies and five-phase permanent magnet synchronous machines. *Mathematics and Computers in Simulation*. 2019; 158: 148–161.
- [10] Hosseini. A, Trabelsi. R, Iqbal. A, Mimouni. M.F.. Comparative study of adaptive sliding mode and resonant controllers in fault tolerant five-phase permanent magnet synchronous motor drive. *The International Journal of Advanced Manufacturing Technology* 2018 ; 96: 2195–2213.
- [11] Záskalický. P. Mathematical model of a five-phase voltage-source PWM-controlled inverter. *Electrical Engineering*. December 2017, Volume 99, Issue 4, pp 1179–1184.
- [12] Schreier. L, Bendl. J, Chomat. M. Operation of five-phase induction motor after loss of one phase of feeding source. *Electrical Engineering*. March 2017, Volume 99, Issue 1, pp 9–18.
- [13] Iqbal. A, Singh. G.K, Pant. V. Some observations on no-load losses of an asymmetrical six-phase synchronous machine. *Turk J Elec Eng & Comp Sci* 2016; 24: 4497-4507.
- [14] Barik. S.K, Jaladi. K.K. Five-Phase Induction Motor DTC-SVM scheme with PI Controller and ANN controller. *Procedia Technology* 2016; 25: 816 – 823

- [15] Arahah MR, Barrero F, Durán MJ, Ortega MG, Martín C. Trade-offs analysis in predictive current control of multi-phase induction machines, *Control Engineering Practice* 2018; 81:105-113.
- [16] Arahah MR, Duran MJ. PI tuning of five-phase drives with third harmonic injection. *Control Engineering Practice* 2009; 17: 787-797.
- [17] Boudjema Z, Taleb R, Djeriri Y, Yahdou A. A novel direct torque control using second order continuous sliding mode of a doubly fed induction generator for a wind energy conversion system. *Turk J Elec Eng & Comp Sci* 2017; 25: 965-975.
- [18] Ouassaid M, Elyaaloui K, Cherkaoui M. Sliding Mode Control of Induction Generator Wind Turbine Connected to the Grid. *Advances and Applications in Nonlinear Control Systems*. 2016. 635:531-553
- [19] Monmasson. E, Louis. J.P. Presentation of a control law for IM drive based on the dynamic reconfiguration of a DTC algorithm and a SVM-DTC algorithm. *Mathematics and Computers in Simulation*. 2003; 63: 321-333.
- [20] Sandre-Hernandez . O, Rangel-Magdaleno. J, Morales-Caporal. R, Bonilla-Huerta. E. HIL simulation of the DTC for a three-level inverter fed a PMSM with neutral-point balancing control based on FPGA. *Electrical Engineering*. September 2018, Volume 100, Issue 3, pp 1441-1454.
- [21] Khedher. A, Mimouni. M.F. Sensorless-adaptive DTC of double star induction motor. *Energy Conversion and Management* 2010; 51: 2878-2892.
- [22] Ammar. A, Benakcha. A, Bourek. A. Closed loop torque SVM-DTC based on robust super twisting speed controller for induction motor drive with efficiency optimization. *international journal of hydrogen energy* 2 0 1 7; xxx: 1-3
- [23] Pimkumwong. N, Wang. M.S. Full-order observer for direct torque control of induction motor based on constant V/F control technique. *ISA Transactions* 2018; 73: 189-200.
- [24] Mesloub. H, Boumaaraf. R, Benchouia. M.T, Goléa. A, Goléa. N, Srairi. K. Comparative study of conventional DTC and DTC SVM based control of PMSM motor - simulation and experimental results. *Mathematics and Computers in Simulation*. 2018; 63: 321-333.
- [25] Morel. F, Retif. J.M, Lin-Shi. X, Valentin. C. Permanent Magnet Synchronous Machine Hybrid Torque Control. *IEEE transactions on Industrial Electronics* 2008; 55: 501-511.
- [26] X Lin-Shi, F Morel, A Llor, B Allard, J M Rétif. Implementation of Hybrid Control for Motor Drives. *IEEE Transactions on Industrial Electronics* 2007; 54: 1946-1952.
- [27] Lin-Shi X. Commande des systèmes de conversion d'énergie. Habilitation à diriger des recherches. *Institut National des Sciences Appliquées de Lyon* juillet 2007.
- [28] Morel F, Lin-Shi X, Rétif JM, Allard B. A predictive current control applied to a permanent magnet synchronous machine, comparison with a classical direct torque control. *Electric Power Systems* 2008; 78: 1437-1447.
- [29] Retif JM, Lin-Shi X, Llor AM, Morand F. New Hybrid Direct-Torque Control for a Winding Rotor Synchronous Machine. *IEEE Power Electronics Specialists Conference* 2004
- [30] Morel F, Retif JM, Lin-Shi X, Llor AM. Fixed Switching Frequency Hybrid Control for a Permanent Magnet Synchronous Machine. *IEEE International Conference on Industrial Technology* 2004.
- [31] Arichi F, Gorp JV, Djemai M, Defoort M, Cherki B. Hybrid state estimation for a class of switched system using Petri Nets. *European Control Conference* 2014
- [32] Elmetennani S, Laleg-Kirati TM, Djemai M, Tadjine M. New MPPT algorithm for PV applications based on hybrid dynamical approach. *Journal of Process Control* 2016; 48: 14-24.
- [33] Gorp JV, Giua A, Defoort M, Djemai M. Active Diagnosis for Switched Systems Using Mealy Machine Modeling. *Diagnosability, Security and Safety of Hybrid Dynamic and Cyber-Physical Systems* 2018. 147-173
- [34] Djondiné P, Barbot JP, Ghanes M. On the Petri Nets Control of the Multicellular Converter. *International Journal of Emerging Technology and Advanced Engineering* 2017; 7: 332-336.
- [35] Liu X, Stechlini P. Switching and impulsive control algorithms for nonlinear hybrid dynamical systems. *Nonlinear Analysis: Hybrid Systems* 2018; 27: 307-322.
- [36] Halbaoui K, Belazreg MF, Boukhetala D, Belhouchat MH. Modeling and Predictive Control of Nonlinear Hybrid Systems Using Mixed Logical Dynamical Formalism. *Advances and Applications in Nonlinear Control Systems*. 2016. 635:421-450
- [37] Djondiné P, Barbot JP, Ghanes M. Comparison of Sliding Mode and Petri Nets Control for Multicellular Chopper. *International Journal of Nonlinear Science* 2018; 25: 67-75.
- [38] Defoort M, Gorp JV, Djemai M. Multicellular Converter: A Benchmark for Control and Observation for Hybrid Dynamical Systems. *Hybrid Dynamical Systems* 2015 293-313
- [39] Benmiloud M, Benalia A. Hybrid Control Scheme for Multicellular Converter. *IEEE 2013 International Conference on Control, Decision and Information Technologies (CoDIT)*; 476-482
- [40] Benmansour K, Benalia A, Djemai M, Leon J. Hybrid control of a multicellular converter. *Nonlinear Analysis: Hybrid Systems* 2007; 1: 16-29.
- [41] Semail E. Entrainements Electriques Polyphasés: vers une approche système. *Rapport de L'Habilitation à Diriger des Recherches, Université des Sciences et Technologies de Lille* 2009.
- [42] Jones M, Satiawan INW. A simple multi-level space vector modulation algorithm for five-phase open-end winding drives. *Mathematics and Computers in Simulation* 2013; 90: 74-85
- [43] Toliyat, HA.. Analysis and simulation of multi-phase variable speed induction motor drives under asymmetrical connections. *In Applied Power Electronics Conference and Exposition* 1996; 2:586-592.
- [44] Vizireanu D, Brisset S, Kestelyn X, Brochet P, Miletet Y, Laloy D. Investigation on multi-star structures for large power direct-drive wind generator. *Electric Power Components and Systems* 2007; 35:135-152.
- [45] Kesraoui.H, Benelghali .S, Trabelsi.R, Mimouni. M.F, Outbib.R. Control Of Tow Five-Phase Synchronous Machine Series Connected Supplied Through A Five Arms Inverter With Alternate Mode. *IEEE 2014 International Conference on Electrical Sciences and Technologies in Maghreb (CISTEM)*
- [46] Guzman. H, Duran. M.J, Barrero.F, Toral. S. Fault-tolerant current predictive control of five-phase induction motor drives with an open phase. *37th Annual Conference of the IEEE Industrial Electronics Society* 2011.